Granular Matter (2005)
DOI 10.1007/s10035-005-0203-4

ORIGINAL PAPER

Ashutosh Trivedi · Vijay Kumar Sud

Ultimate bearing capacity of footings on coal ash

Received: 16 August 2004 / Published online: 14 June 2005

Abstract Coal ash is recognized as an alternative fill material to the conventional natural soils near a coal fired thermal power station where its large deposits are available. This paper presents experimental investigations on footings on coal ash subjected to loads. A series of laboratory model tests on varying sizes of footings were conducted. The conventional bearing capacity evaluation methods applied for natural soils do not consider progressive failure. These effects are explained based on the non-linear strength behavior of the granular soil and occurrence of progressive failure. The classical bearing capacity theory was applied in relation to the relative dilatancy of coal ash to describe this phenomenon. Few novel observations presented here show that the extent of progressive failure of ash fills is a compressed function of material characteristics of the ash, size and depth of footing and the settlement ratio.

Keywords Coal ash · Plate load test · Relative density · Relative dilatancy · Bearing capacity · Settlement ratio

1 Introduction

Coal ash is an industrial byproduct of the combustion of coal in thermal power stations. Its chemical composition depends upon the variety of coal produced in various parts of the world. The quality of the coal mass varies from one mine to another. Therefore, differences are apparent among the ashes. In the burning chamber, pulverized coal powder is fired where its decomposition occurs. During combustion, as the coal passes through the high temperature zone in the furnace, volatile matter and carbon are burned off while most of mineral impurities melt. The fused matter is quickly transported to lower temperature zones, where it solidifies as spherical particles of glass. Some of the mineral matter agglomerate forms bottom ash, but most of it flies out with the flue gas stream, which is called fly ash. Coal ash is subsequently removed from the gas by electrostatic precipitators (ESPs).

Coal ash containing less than 10% lime is normally a product of combustion of anthracite, bituminous, and subbituminous coal. In the furnace, when large spheres of molten glass are not cooled rapidly, sillimanite ($Al_2O_3.SiO_2$) or mullite ($3Al_2O_3.SiO_2$) crystallizes as slender needles in the interior of the glassy spheres. The study of x-ray diffraction of Ropar ash has confirmed presence of quartz, mullite, and hematite or magnetite [1]. These crystalline minerals are normally non reactive at ordinary temperatures. The absence of peaks associated with hydrated silicates in diffraction analysis of coal ashes provides a basis for its treatment as a cohesionless material [2]. Further, the absence of active lime and clay minerals allows coal ash to be considered as a granular, cohesionless geo-material. Several investigators namely Cunningham et al. [3], Toth et al. [4], and Seals et al. [5] reported similar results on ashes procured from different parts of the world. Normally the basic soil characteristics can be established from laboratory tests on undisturbed samples but for coal ash, the problem of sample disturbance generally prevents this approach from being used. Therefore, testing under controlled conditions of density and overburden has been developed as the most efficient means of verifying and establishing correlations for cohesionless ashes.

Several plate load tests have been carried out on large controlled samples to monitor density, overburden, and applied stress. A large number of standard size reconstituted ash samples has been sheared under drained conditions in a triaxial

A. Trivedi (✉)
House No.8, Type V,
Delhi College of Engineering, Bawana Rd.,
Delhi-110042, India
E-mail: atrivedi@civil.dce.edu

A. Trivedi
Department of Civil Engineering,
Delhi College of Engineering,
Bawana Road, Delhi-110042, India
Tel.: 91(11)27871043,44,45, Ext. 1522(O), 2527(R),
919811426120 (Mo)

V. K. Sud
Department of Civil Engineering,
Thapar Institute of Engineering
& Technology (Deemed University),
Patiala-147004, India

apparatus to find constitutive relationships for peak friction angle on the basis of knowledge of relative density, mean effective confining pressure, and critical state friction angle. The drained conditions ensure that during the shearing operation no pore pressures develop in the sample and the strength parameter correspond to the effective angle of friction.

1.1 Review of previous work

Coal ash is disposed off hydraulically in the form of slurry in ash ponds constructed near a thermal power plant. These are generally loose deposits, which make the fill unstable. Ash dikes restrict the side flow of ash slurry. In order to improve its engineering properties, ash is compacted in layers using vibratory compactor. Standard penetration test result on hydraulically deposited ash indicates very low values of N [3]. The standard penetration test is a widely used technique for soil investigation. It involves the measurement of cutting resistance offered by the soil to the penetration of standard split spoon barrel for 45 cm against a number of blows of a fixed weight hammer out of which the resistance offered to the first 15 cm of penetration is rejected. The resistance is recorded in terms of a number of blows (N) required for 30 cm of penetration at selected depth (normally at 1 or 1.5 m each). It is corrected for various losses besides the corrections for overburden and water table. Toth et al. [4] reported a wide variation ($N = 10 - 55$) in standard penetration resistance of Ontario ash, which might be due to the presence of varied grain sizes and density states.

The static cone penetration test is yet another widely relied technique for soil investigation. Static cone penetration test is normally conducted using a cone (area of cone base, $A_c = 9.97\,cm^2$), with apex angle of 60° and removable friction sleeve (area of sleeve surface, $A_s = 148\,cm^2$). The extension rod is pressed in alignment into fill at a rate of 20 mm/sec to measure the cone tip force (Q_c) and total force (Q_t). Cone with friction sleeve is pushed into the ash next to estimate total force (Q_t). The average of point force and total force recorded at a depth is used to calculate the cone tip resistance ($q_c = Q_c/A_c$), frictional resistance ($q_f = (Q_t - Q_p)/A_s$), and friction ratio ($f = q_f/q_c$).

Seals et al. [5] reported static cone penetration tests results on compacted ash fill where the average friction ratios for ash (3–4.7%) was appreciably higher than the value (2%) reported by Schmertmann [6] for clayey silts, sand mixes, silty sands, silts, and fine sands. The investigations carried out by Cousens and Stewart [7] for the range of cone resistance and percent friction ratio (0–200 kPa and 0–8% respectively) indicated grain sizes in the range of silt (60–80%) and clay (5–10%). The record of variation in friction ratio may be useful in characterization of ashes procured from different sources compared to soils. A higher record of friction ratio is normally interpreted as a greater resistance in side friction for a pile foundation. Trivedi and Singh [8] reported higher load bearing capacity of shallow foundations on ash fills than actually estimated by cone resistance.

Leonards and Bailey [9] suggested that interpretation of load settlement relations for foundation on compacted ash from standard penetration tests or static cone penetration tests may be erroneous because of the inadequacy of these tests to sense the effect of prestressing due to compaction. They emphasized that the plate load testing technique may alone be relied to interpret the load bearing behavior of ash fills. The static cone penetration resistance may be regarded as successive bearing capacity failures of a small conical footing on ash. While in the plate load test better control in the size and the shape of the footings may be put into practice.

1.2 Interpretation of bearing capacity of small footing

The bearing capacity of a footing on a geomaterial is generally evaluated at shallow depths using the bearing capacity factors N_c and N_q proposed by Prandtl [10] and Reisner [11] respectively. However, substantial differences have been reported in the semi-empirical bearing capacity factor for shallow foundations N_γ in numerous studies [12–18].

The classical bearing capacity equation for strip foundations, popularly known as the Terzaghi formula, is given by

$$q_{ult} = c' N_c + \sigma'_{ov} N_q + 0.5 N_\gamma \gamma' B \tag{1}$$

where c' is the effective soil cohesion intercept, σ'_{ov} is the overburden acting at the footing base expressed in terms of effective stress, γ' is the buoyant unit weight, and B is the footing width.

For cohesionless materials the above equation is represented as

$$q_{ult} = \sigma'_{ov} N_q + 0.5 N_\gamma \gamma' B \tag{2}$$

$$N_q = \tan^2(\pi/4 + \phi'/2) e^{\pi \tan \phi'} \tag{3}$$

The bearing capacity does not increase linearly with the width of the footing or overburden contrary to that obtained from Equation (2). This phenomenon is called the scale effect by de Beer [19,20] who attributed this to the nonlinear shape of the soil failure envelope resulting in the secant measure of the friction angle, which decreases with mean effective confining stresses. With increasing confinement, dense and loose cohesionless soils have much less marked difference in peak angle of internal friction. This effect is more pronounced in geomaterials such as coal ash that suffer from progressive crushing. The progressive crushing is a phenomenon observed in the stressed granular media where the increasing stresses gradually deform the particle to break and finally to crush. McDowell and Bolton [21] have provided additional data that support reduction in the peak angle of friction at the pile tip in case of high overburden pressure and relative density.

Equation (2) may be expressed for a footing of any shape as

$$q_{ult} = \sigma'_{ov} N_q S_q + 0.5 N_\gamma S_\gamma \gamma' B \tag{4}$$

S_q and S_γ are the empirical shape factors.

For the surface footing Equation (4) may be rewritten as

$$q_{ult} = 0.5 N_\gamma S_\gamma \gamma' B \tag{5}$$

Using a concept proposed by Vesic [16] and Chen [17] N_γ may be put forward as

$$N_\gamma = 2(1 + N_q)\tan\phi' \quad (6)$$

$$N_\gamma = 2(1 + N_q)\tan\phi'\tan(\pi/4 + \phi'/5) \quad (7)$$

Experimentally it is obtained as,

$$N_\gamma = q_{\text{ult}}/0.5\gamma' B \quad (8)$$

The conventional shape factor (S_γ) is not applied in the relative dilatancy approach. Some investigators have suggested modification in the bearing capacity factor N_γ for the roughness of the base contact surface [22]. The use of a common plate material footing base device throughout the testing program allowed the authors to interpret the effect of base roughness of the contact surface as a common factor grouped in the ratio of experimental values of N_γ obtained from the angle of internal friction. Since ϕ varies as the state of stress, density and material characteristics of the soil, the concept of stress dilatancy enunciated by Rowe [23], advanced by de Josselin de Jong [24] and Bolton [25] is utilized.
Bolton proposed the empirical equation

$$\phi_{\text{peak}} = \phi_{\text{cr}} + AI_{\text{r}} \quad (9)$$

$$\text{where } I_{\text{r}} = RD(Q - \ln p') - r \quad (10)$$

where A is an empirical constant and has the value of 3 for axisymmetrical and 5 for plane strain case; I_r is the relative dilatancy index; p' is the mean effective confining pressure in kPa; RD is relative density; and Q and r are empirical material fitting constants with values of 10 and 1, respectively, for clean silica sand. The dilatancy increases with increasing Q and decreases with increasing r (Salgado et al [26]). Incorporating Billam's [27] triaxial test data, Bolton [25] suggested that progressive crushing suppresses dilatancy in the soils with weaker grains, i.e. limestone, anthracite, and chalk, which show Q values of 8, 7, and 5.5, respectively. The Ropar ash, which may be classified as ASTM class F ash, contains a substantial amount of crystalline fine silica grains followed by alumina and the oxides of iron, calcium, and magnesium. It shows a Q as low as 7.7 [28, 2]. This occurs mainly because of reduction of the critical mean confining pressure beyond which increase in mean confining pressure for a relative density does not increase peak angle above the critical angle. Perkins and Madson [29] proposed to integrate this approach of progressive failure with the bearing capacity of shallow foundations on sand. This approach is presently modified and extended to meet the requirements of the ash fills.

2 Experimental methods

The experimental methods consisted of chemical and physical analysis of ash procured from a thermal power plant at Ropar, Punjab, India. To serve a micromechanical purpose the oven dry ash sample was scanned by an electron microscope at 1000 X. The wet chemical and X-ray diffraction analysis of incombustibles in the ash was conducted to find out the chemical and mineralogical composition. The grain size analysis of the dry ash sample was conducted by the mechanical sieve method. For the fraction passing the 75-μm sieve, a hydrometer method was employed separately.

The ash was deposited in loose lift of 150 mm in a square trench of 1.5 m side and 1.5 m deep (Figure 1(a)). It was compacted by a precalibrated plate vibrator mounted on a flat rectangular plate (152 mm × 390 mm). The rating of the plate vibrator was 2950 rpm. A constant magnitude of vibration was required to achieve the desired relative density. The trench was filled up in layers maintaining constant density throughout. The density checks were applied at regular intervals along with the trench filling operation using thin core cutter sampling and penetration of an 11 mm diameter needle penetrometer under a constant pressure (Figure 1 (b)).

After filling ash up to a desired level, plate load test was initiated on compacted ash. The plate load test was conducted on the ash fill by a hydraulic jack. Model tests were conducted for surface footings of varying sizes namely 0.1, and 0.125 m wide strip and 0.3 m squares in dry as well as submerged conditions for two different ashes and a sand. A few of the experiments were conducted for embedded footings at unit depth to width ratio. Additionally in situ density checks and laboratory shear tests were also conducted. The displacement of the plate was monitored using pre-calibrated settlement gauges of least count 0.01 mm. The total assembly including hydraulic jack, proving ring and the plate was aligned with the help of a plumb bob to attain verticality.

2.1 Density checks on compacted ash fill

A needle penetrometer [8] was used to verify the relative density of compacted ash in the test trench (Figure 1 b). This consists of a graduated and smooth glass tube of 11 mm external diameter. The penetration of the needle penetrometer was calibrated at known relative densities. It was used as a probe to ascertain the density state of ash in the trench. A special device was fabricated to monitor the vertical movement of this probe. On the top of the probe, a plate was attached so that a fixed weight could be placed on it. The ash was vibrated in a 3000 ml cylindrical vessel of inside diameter 150 mm under a surcharge of 248 N and at a frequency of 60 Hz. The relative density was interpreted from maximum and minimum density estimates obtained by the weight-volume relationship at vibration intervals of 30 s each. The penetration of the probe under a constant pressure was allowed into the ash at varying relative densities. A typical plot, prepared for the verification of relative density with depth of penetration of the needle is shown in Figure (3). However, for low relative densities the estimates of density were based solely upon the weight-volume relationship.

3 Interpretation of results

3.1 Characterization

Micrographic observations of Ropar ash [2] suggested the existence of siliceous aluminous particles (brownish glass

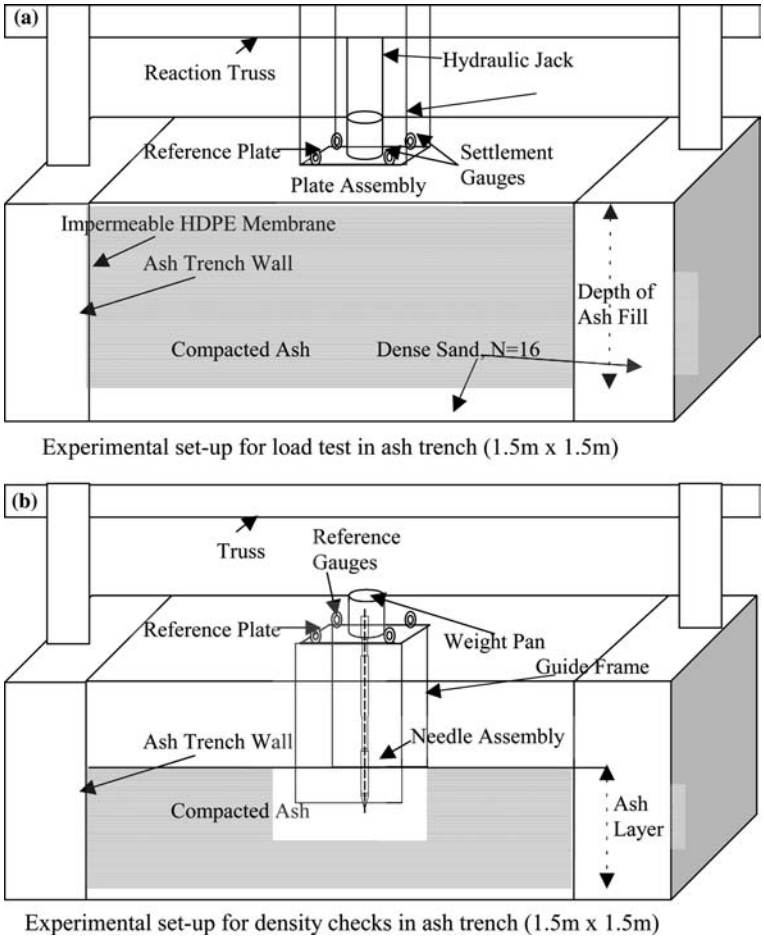

Fig. 1 (a) Experimental set-up for load test in ash trench (1.5 m × 1.5 m) (b) Experimental set-up for density checks in ash trench (1.5 m × 1.5 m)

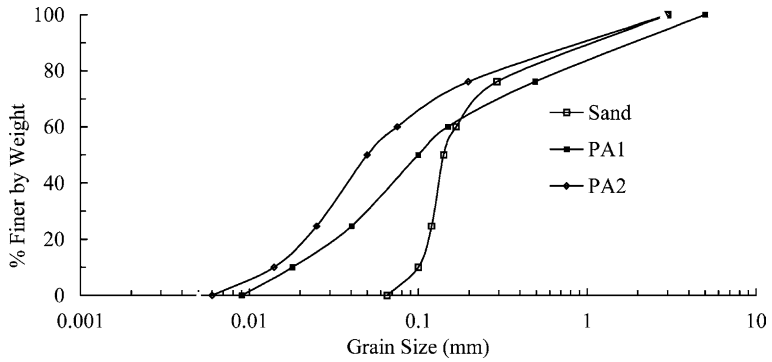

Fig. 2 Grain size distribution curves of coal ashes and test sand

spherules), rounded porous grains (white sponge like grains), agglomerated glass spherules (reflecting), magnetite (dark gray), hematite (dirty red), irregular porous grains of carbon (black) in Ropar ash. The mechanical properties of ash depend mainly upon the grain size, shape, and distribution; however, in order to ascertain the precise chemical composition of the Ropar ash wet chemical analysis was conducted. The Ropar ash used in the present study has SiO_2 (57.5%), Al_2O_3 (27.2%), Fe_2O_3 (5.4%), nonreactive CaO (3.1%), MgO (0.4%), soluble material (<1%), and unburned carbon (∼4%) by weight.

3.2 Grain size and specific gravity

Figure (2) shows the grain size analysis of coal ashes designated as A1, A2 and typical sand used in this study. The sand was employed in the separate small-scale load test to check

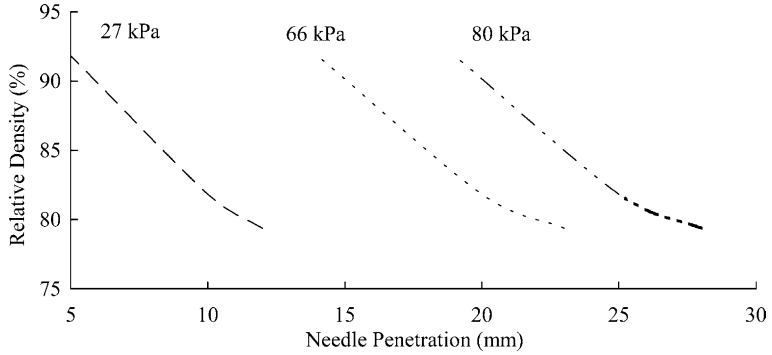

Fig. 3 Relative densities vs.needle penetration at constant pressure for coal ash

Table 1 Summary of experimental program

Ash type	RD (%)	Test conditions	Size (m)	Footing	D/B	No. of tests
A1	58.7, 65.9, 80	Compacted dry,	0.1	Strip	0,1	12
	65.9, 80	submerged	0.1	Strip	0	4
	58.7, 65.9, 80	Compacted dry	0.125	Strip	0,1	12
A2	50, 65, 75.9, 81.9	Compacted dry,	0.1	Strip	0,1	16
	81.9	submerged	0.1	Strip	0	2
	65, 75.9, 81.9	Compacted dry	0.125	Strip	0,1	12
A2	27.5, 45.3	Compacted dry,	0.3	Square	0	4
	27.5, 45.3	submerged	0.3	Square	0	4
Sand	-	Compacted dry,	0.1	Strip	0	2
		submerged	0.1	Strip	0	2

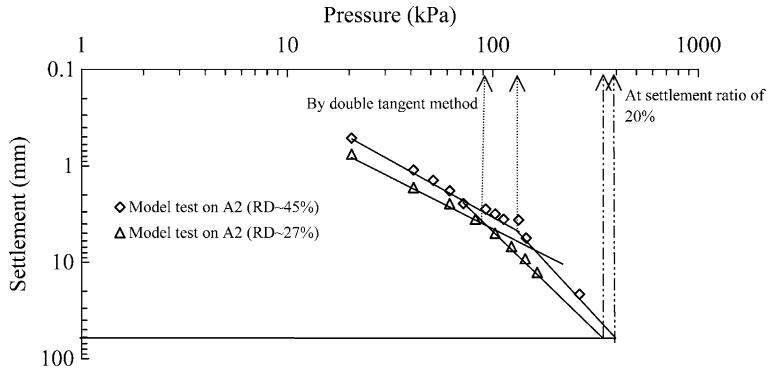

Fig. 4 A typical pressure settlement plot for determination of failure load by double tangent and 20% settlement ratio for a 0.3 m square plate

reproducibility of the results for sand. The ashes consist of grain sizes corresponding to well-graded sandy silt. These grain sizes are classified as non-collapsible ashes on submergence that allows its use as a structural fill [30]. The coal ash has low specific gravity (1.98) compared to sand (2.6).

3.3 Interpretation of bearing capacity

The load capacity of ash fill was estimated by conducting load tests using various sizes of plates (0.1, 0.125 and 0.3 m wide) on two ashes (namely A1 and A2) on varying relative density; for surface footings and footings placed at depth ($D/B = 0, 1$). A summary of the experimental program is given in Table (1). The average of at least two tests was considered to reach a common load settlement plot if the values were within the range of 10%. The typical pressure settlement plots are shown in Figure (4). The pressure settlement plots have varying stages of implicit failure at each data point. It may be understood that at a low settlement ratio (S/B) only limited failure is initiated. The settlement ratio is defined as a ratio of settlement (S) to the width of the footing (B). A selected value of q_{ult} at a low settlement ratio (S/B) has a magnitude of p' such as a result of a high-mobilized angle of internal friction. With the progress of settlement the failure surface penetrate deeper in to the ash where mean effective stress p' increases. This process continues until the entire failure surface reached the widely described mobilized strength at an extended loading when the settlement ratio might be in the excess of 20%. In the present study, the ultimate bear-

ing capacity is evaluated by the classical double tangent [16] method and at a settlement ratio of 20% on an extended plot.

A series of shear tests conducted on compacted ash samples indicates that shear strength is mainly derived from frictional properties [28]. In a triaxial shear test, the peak angle of internal friction was obtained corresponding to various relative density (RD) and mean effective confining pressure (p'). The critical state friction angle was obtained by shearing an ash sample to axial strains in excess of 25%. The critical state friction angle (ϕ_c), a morphological mineralogical parameter, was observed to be 30° for Ropar ash. The value of parameter Q for coal ash was obtained as 7.7 [2]. Therefore the knowledge of ϕ_c, RD, and p' is utilized to interpret the peak angle of internal friction of ash from Equation (11) as

$$QRD - r = (\phi'_p - \phi_c)/A + RD\ln(p') \tag{11}$$

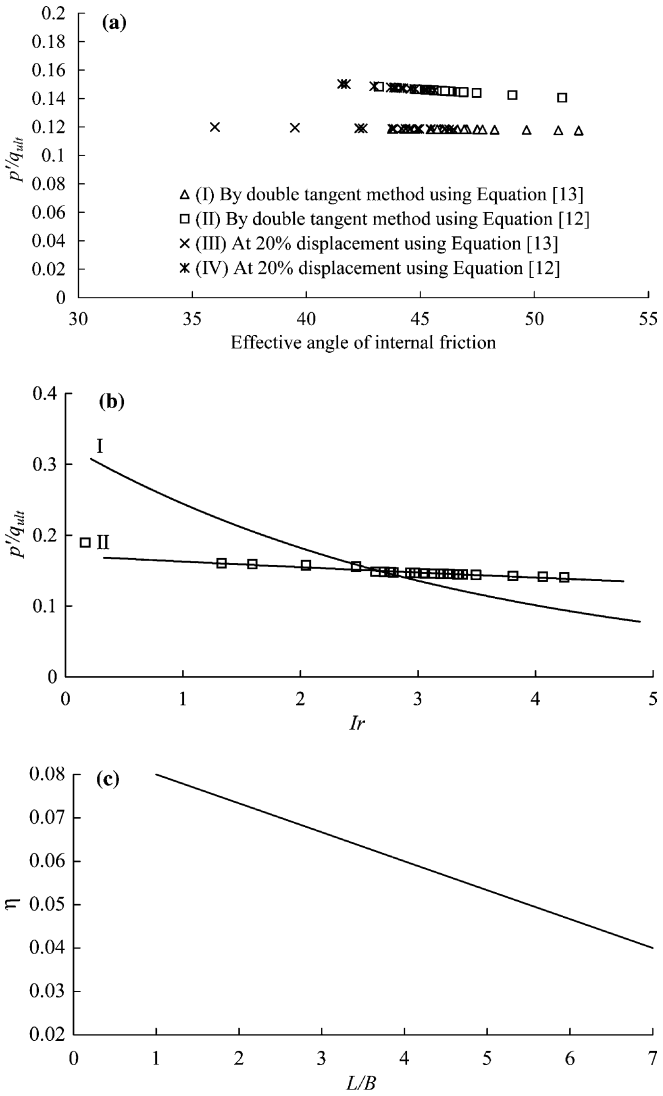

Fig. 5 (a) p'/q_{ult} versus peak friction angle for coal ash (b) p'/q_{ult} vs. Ir (c) η vs. L/B

where ϕ'_p and ϕ_c are peak effective and critical angles of friction, and Q and r are material fitting parameters for coal ash. The angle of internal friction obtained from Equation (11) is substituted from an expression for p'/q_{ult} obtained subsequently by Equation (12) or (13). Figure (5a) shows the relationship of effective mean confining pressure (p') with friction angle. Taking into account the progressive failure, the values of p'/q_{ult} may be drawn with the index of relative dilatancy (Figure 5b). The expression suggested by de Beer [20] provides a traditional estimate of p'. Considering the effect of overburden p'/q_{ult} may be evaluated using concepts of de Beer [20] as

$$p'/q_{ult} = \eta(1 + 3\sigma'_{ov}/q_{ult})(1 - \sin\phi')/4 \tag{12}$$

where q_{ult} is the ultimate bearing capacity of a footing. The value of η varies with L/B ratio where L is the length and B is the width of the footing as shown in Figure (5c). σ'_{ov} is effective overburden pressure.

Perkins and Madson [29] proposed an expression on the basis of nonlinear limit plastic analysis, which might be used with an advantage for consideration of a slip failure corresponding to an invariant (mean confining pressure) and effective friction angle.

$$p'/q_{ult} = \eta 3.1\exp(-0.073\phi') \tag{13}$$

where q_{ult} is ultimate bearing capacity of a footing. The value of η varies linearly from 0.04 for plane strain footing case to 0.08 for axi-symmetrical case as shown by a line in Figure (5c).

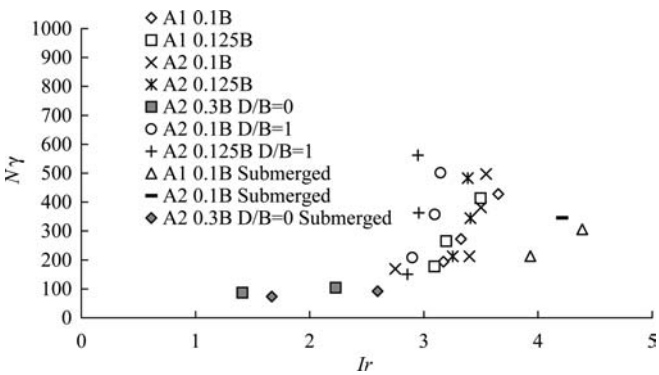

Fig. 6 Experimental value of N_γ by double tangent method vs. Ir

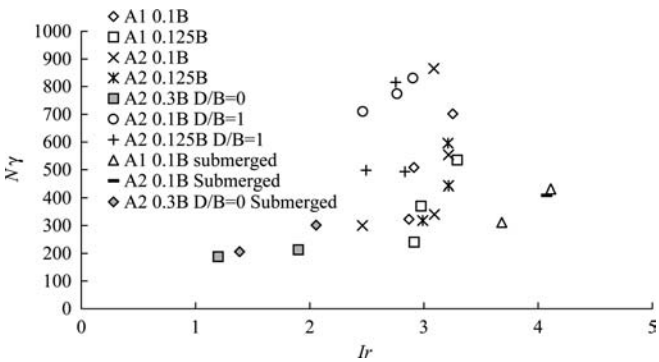

Fig. 7 Experimental value of N_γ at a settlement ratio of 20% vs. Ir

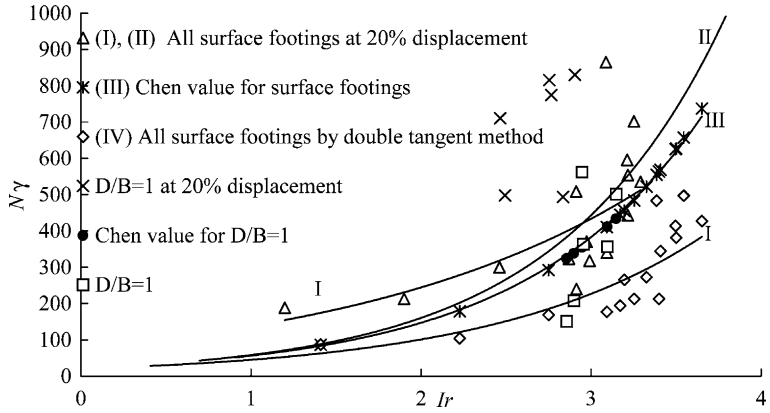

Fig. 8 Experimental value of N_γ compared for double tangent method at a settlement ratio of 20% and theoretical value by Chen for surface footings vs. *Ir*

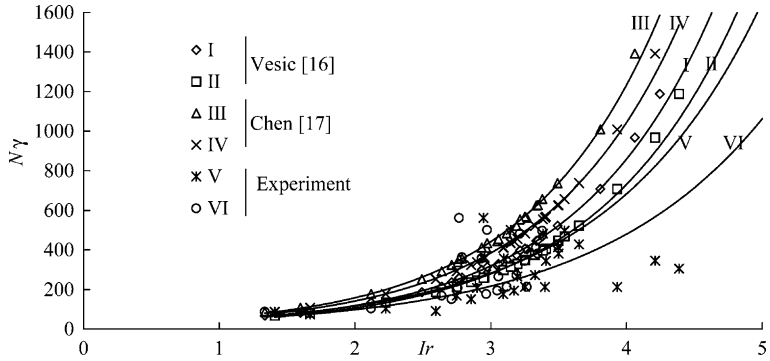

Fig. 9 Comparison of bearing capacity factor by double tangent using various schemes vs. *Ir*

3.4 The bearing capacity factor

The experimental values of bearing capacity factor N_γ were obtained using Equation [8]. It is compared with the values of N_γ obtained from composite consideration of Ir. The mobilized peak effective angle of internal friction that is a function of mean confining pressure (p') and relative density was evaluated as per Equation [11]. Further the mean confining pressure corresponding to a load test is a function of ultimate load and average mobilized peak effective angle of internal friction as per Equation [12] and [13] respectively. Through a simple computer program the mobilized peak effective angle of internal friction and p' ware obtained at 100 iterations. Based on knowledge of peak effective angle of internal friction the value of Ir may be computed as per Equation [8] and [9].

Figure (6) and (7) show comparison of N_γ obtained from experimental q_{ult} for various sized footings on different ashes placed at surface and at a depth for dry as well as submerged ash fills. The q_{ult} values for Figure (6) were obtained by the classical double tangent method which involved values at intersecting tangents one at the beginning of load settlement plot and that at a point of plot when the three successive equal incremental loads result in to increasing incremental settlement pattern as shown by the intersection of straight lines in log-log plot (pressure vs. settlement) in Figure (5). The method for obtaining q_{ult} values at a settlement of 20% for N_γ in Figure (7) was as per the pattern shown in Figure (4). Considerable gains in understanding may be achieved by analyzing the trend in the experimental N_γ in Figure (6) and (7). The values corresponding to submergence might have greater uncertainties owing to lesser control on relative density. Figure (8) shows trend lines for experimental data points corresponding to surface footings at 20% settlement ratio and at double tangent points. It illustrates a relative nearness of the trend line at 20% settlement ratio to the trend line for Chen's value (Equation 7). Figure (9) demonstrates the comparison of the theoretical N_γ (by Vesic and Chen respectively, as given in Table 2 by reference plots *I*, II and III, IV respectively) and experimental N_γ (at q_{ult} by double tangent method) estimated using schemes for evaluation of Ir(I) by Parkins and Madson [29] and Ir(II) by de Beer [20] as given in Table 2). It is understood that minimum value of N_γ may be picked up as 21 at a low settlement ratio such as corresponding to that obtained by double tangent method. It provides enough cues to support that Chen values are more or less satisfactorily applied to surface footings with significant departures from experimental values for footings at depth.

Figure (10) shows the comparison of bearing capacity factor for peak mobilized friction at corresponding relative density, experimental by double tangent method, and at constant volume friction with variation of Ir. The bearing capacity

Table 2 Summary of important results

Reference figure	Reference plot	Equation	R^2	Supplementary references
5(a)	I	$p'/q_{ult} = 0.1256\ e^{-0.0013\phi'}$	1	By double tangent
	III	$p'/q_{ult} = 0.8725\ e^{-0.0436\phi'}$	0.7134	At 20% settlement ratio Perkins and Madson [29]
	II, IV	$p'/q_{ult} = 0.2\ e^{-0.007\phi'}$	0.9986	de Beer [20]
5(b)	I	$p'/q_{ult} = 0.329\ e^{-0.2969\,Ir}$	0.7105	p'/q_{ult} vs. Ir (I)
	II	$p'/q_{ult} = 0.171\ e^{-0.0498\,Ir}$	0.9222	p'/q_{ult} vs. Ir (II)
5(c)	–	$\eta = [0.52\text{-}0.04L/B]/6$	–	Perkins and Madson [29]
8	I	$N_\gamma = 77.64\ e^{0.5734\,Ir}$	0.5579	At 20% settlement ratio
	II	$N_\gamma = 21e^{1.0167\,Ir}$	0.2114	At fixed intercept
	III	$N_\gamma = 21.61e^{0.9585\,Ir}$	0.9988	Chen [17]
	IV	$N_\gamma = 21.31e^{0.7897\,Ir}$	0.7634	By double tangent method
9	I	$N_\gamma = 16.387e^{0.9896\,Ir}$	0.9971	N_γ Vesic vs. Ir (II)
	II	$N_\gamma = 15.576e^{0.9621\,Ir}$	0.9958	N_γ Vesic vs. Ir (I)
	III	$N_\gamma = 20.249e^{1.0273\,Ir}$	0.9973	N_γ Chen vs. Ir (II)
	IV	$N_\gamma = 19.206e^{0.9987\,Ir}$	0.9961	N_γ Chen vs. Ir (I)
	V	$N_\gamma = 20e^{0.7944\,Ir}$	0.4358	Experimental N_γ vs. Ir (I)
	VI	$N_\gamma = 20e^{0.8827\,Ir}$	0.5033	Experimental N_γ vs. Ir (II)
11(a)	*I*	$Ipr = 0.0753\ Ir + 0.68$	0.2891	At 20% settlement ratio vs. Ir (II)
	II	$Ipr = 0.1105\ Ir + 0.51$	0.3464	By double tangent method vs. Ir (II)
11(b)	*I*	$Ipr = 0.0787\ Ir + 0.65$	0.3122	At 20% settlement ratio vs. Ir (I)
	II	$Ipr = 0.1253\ Ir + 0.43$	0.3612	By double tangent method vs. Ir (I)
	III	$Ipr = 0.044\ Ir + 0.65$	–	Perkins and Madson [29]

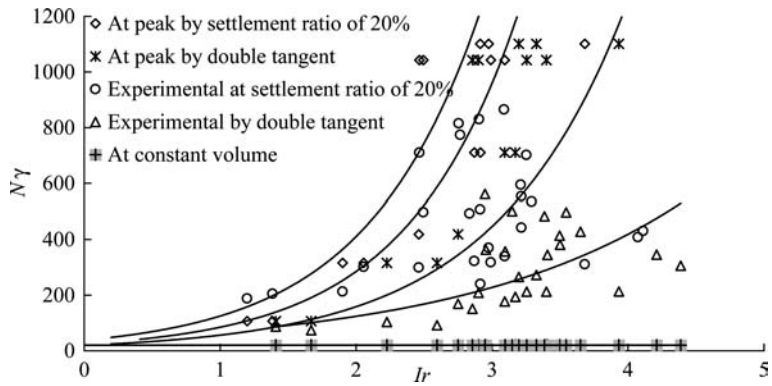

Fig. 10 Comparison of bearing capacity factor for peak experimental and constant volume friction

factor for the ash fills was observed to fall between the estimates by the use of the peak friction and the constant volume or critical angles. The advantage of using the present method is doing away with empirical depth and shape factors that seem to be more speculative for large sizes of footing. Figure (11a) and (11b) show the variation in the index of progressive failure (I_{rp}) with relative dilatancy index obtained using Equation [12] and [13] respectively for various footings considered in the present work. It is compared with the trend lines [29] obtained for sandy soils. The index of progressive failure [29] is defined as

$$I_{rp} = [q_{ult(at\ peak)} - q_{ult(experimental)}]/ [q_{ult(at\ peak)} - q_{ult(at\ constant\ volume)}] \quad (14)$$

If I_{rp} takes a value of one, it implies that the constant volume friction governs the ultimate bearing capacity of ash fill while a value of zero indicates that the peak angle of friction is mobilized. It may be identified here that various factors that influence the progressive failure are settlement ratio, relative density, size, depth of the footing, constant volume, peak friction and soil material properties represented by parameters Q and r. The influence of settlement ratio, size and depth of the footing is shown in Figure (11a) and (11b) by arrows. The effect of constant volume friction, the peak friction and soil material property represented by parameters Q and r is implicit in the observed data of ultimate bearing capacity. The effect of relative density should normally be interpreted together with mean effective confining pressure, which is a multi-dependent parameter of size, shape and depth of the footing. Figure (11a) and (11b) show that the effect of increasing size and depth is to suppress dilatancy. For observed ultimate bearing capacity at a high settlement ratio the progressive failure increases irrespective of size and depth of the footing. The index of progressive failure is represented by a curve fitting general equation ($I_{rp} = mIr + n$) where the fitting parameters (m and n) should be interpreted as to have

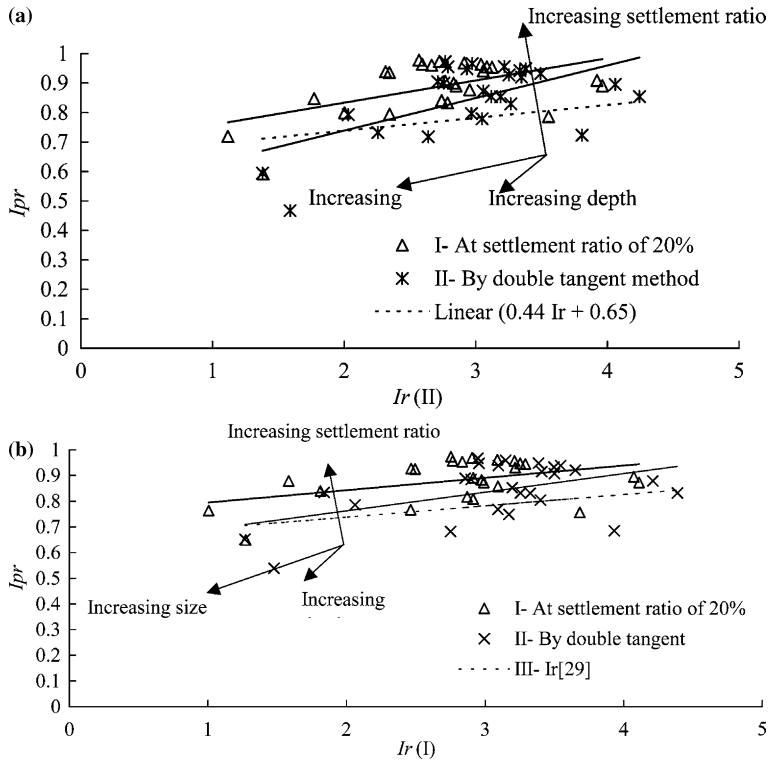

Fig. 11 (a) Extent of progressive failure vs. *Ir*(II) (b) Extent of progressive failure vs. *Ir*(I)

an effect of observed data set and the method employed to estimate *Ir*. The difference in the method employed to estimate *Ir* necessarily incorporates the assumptions involved in the techniques for estimation of effective mean confining pressure.

4 Conclusions

The knowledge of material characteristics, relative density, and mean confining pressure are used to correlate relative dilatancy of the ash with ultimate bearing capacity. The bearing capacity of shallow foundations on ash fill estimated using conventional methods lead to arbitrary estimates because of the absence of the representative parameter for the progressive failure of the ash. This was incorporated by the use of the relative dilatancy index in prediction of ultimate bearing capacity. It was validated using data of the plate load test on coal ash. It is proposed to use the bearing capacity factor as per the magnitude of relative dilatancy. The bearing capacity of ash fill may be directly estimated using the $N_\gamma - Ir$ relationship suggested by the authors. At higher settlement ratio the bearing capacity factor was significantly higher than that estimated by the double tangent method. The settlement ratio is limited to a quantifiable magnitude according to the specifications of the footing. At lower settlement ratio a value of N_γ (=20) may be safely picked up for the bearing capacity calculations. The proposed empirical relation based on the load tests show that the progressive failure of the fill is affected by the material characteristics, size and depth of the footing and the settlement ratio. More research focus would be required to understand how the effective mean confining pressure is quantified as a function of the depth and the size of the footings.

Acknowledgements The study presented here is based on the data set of coal ash from Ropar thermal power plant. All the opinions, findings and conclusions expressed herein are those of the authors, pertain only to the observed data set, and do not necessarily reflect the behavior of all types of coal ashes. The facilities extended to the authors at Delhi College of Engineering, Delhi and TIET, Patiala, India is thankfully acknowledged.

Appendix: List of Notations

ϕ'	effective friction angle (degrees)
γ	unit weight (kNm^{-3})
ϕ_c	constant volume friction or critical friction angle (degrees)
ϕ'_{peak}	effective peak friction angle (degrees)
η	a factor depending upon B/L ratio of the footing
σ'_{ov}	effective overburden pressure (kPa)
A	an empirical constant ; 3.0 for axisymmetrical, 5.0 for plane strain case
L, B, D	length, width, depth of footing (m)
c'	effective cohesion (kPa)
I_r(I)	relative dilatancy index (Perkins and Madson [29])
I_r(II)	relative dilatancy index (de Beer [20])
I_{rp}	index of progressive failure
N_c, N_q, N_γ	bearing capacity factors for shallow footing
p'	mean confining pressure (kPa)
Q, r	empirical material constants
q_{ult}	ultimate bearing capacity (kPa)
RD	relative density
S_q	empirical shape factor

References

1. Trivedi, A.: Engineering behavior of coal ash, Ph.D. Thesis, Dept. Civil Eng., TIET, Patiala, 1999
2. Trivedi, A., and Sud, V.K.: "Grain characteristics and engineering properties of coal ash". Granular Matter, **4**(3): 93–101 (2002)
3. Cunningham, J.A., Lukas, R.G., and Andreson, T.C.: "Improvement of fly ash and stage - A case study". Proc. Conf. Geotech. Practice for Disposal of Solid Waste Materials, ASCE, Ann Arbor, Mich., 227–45 (1977)
4. Toth, P.S., Chan, H.T., and Crag, C.B.: "Coal ash as structural fill with reference to Ontario experience". Can. G.J., Vol. **25**, 594–704 (1988)
5. Seals, R.K., Moulton, L.K., and Kinder, D.L.: "Insitu testing of a compacted fly ash fill". Proc. Conf. Geotech. Practice for Disposal of Solid Waste Materials, ASCE, Ann Arbor, Mich., 493–516 (1977)
6. Schmertmann, J.H.: Guidelines for cone penetration test, performance and design. US Federal Highway Administration, Washington, DC, Report FHWATS-78–209, 145 (1978)
7. Cousens, T.W., and Stewart, D.I.: "Behaviour of a trial embankment on hydraulically placed pfa". Engineering Geology, **70**: 293–303 (2003)
8. Trivedi, A., and Singh, S.: "Cone resistance of compacted ash fill". J. Testing and Evaluation, ASTM International, Vol. **32**(6): 429–437 (2004)
9. Leonards, G.A., and Bailey, B.: "Pulverized coal ash as structural fill". J. Geotech. Eng., ASCE, **108**: GT4, 517–531 (1982)
10. Prandtl, L.: Über die harte plastischer korper (in German). Nachr, Kgl. Ges Wiss Gottingen Math. Phys. K.O.I. Berlin, 74–85 (1920)
11. Reisner, H.: "Zum erddrulk problem", (in German). Proc. Ist Int. Conf. App. Mech., Delft, The Netherlands, 295–311 (1924)
12. Feda, J.: "Research on bearing capacity of loose soil". Proc. 5th Int. Conf. Soil Mech. Found. Eng., Paris, Vol. **1**: 635–642 (1961)
13. Meyerhof, G.G.: " Some recent research on bearing capacity of foundations ". Can.G.J., Vol. **1**(1): 16–26 (1963)
14. Meyerhof, G.G.: "Shallow foundations". J. Soil Mech. Found. Div., ASCE, Vol. **91**: SM2, 21–31 (1965)
15. Brinch Hasen, J.: " A revised and extended formula for bearing capacity". Bulletin No.28, Danish Tech. Inst., Copenhagen, 5–11 (1970)
16. Vesiĉ, A.S.: "Analysis of ultimate loads of shallow foundations". J. Soil Mech. Found. Div., ASCE, Vol. **99**: No. SM-1, 45–69 (1973)
17. Chen, W.F.: Limit analysis and soil plasticity. Elsevier, Amsterdam. 1975
18. Zadroga, B.: "Bearing capacity of shallow foundations on noncohesive soils". J. Geotech. Eng., ASCE, Vol. **120**(11): 1991–2008 (1994)
19. de Beer, E.E.: " The scale effect in the transposition of the results of deep sounding tests on the ultimate bearing capacity of piles and cassion foundations". Geotechnique, **8**(1): 39–75 (1963)
20. de Beer, E.E.: "Bearing capacity and settlement of shallow foundations on sand". Proc. Symposium on Bearing Capacity and Settlement of Foundations, Duke University, Durham, N.C., 15–33 (1965)
21. Mcdowell, G.R., and Bolton, M.D.: "Effect of particle size distribution on pile tip resistance in calcareous sand in the geotechnical centrifuge". Granular Matter, **2**(4): 179–187 (2000)
22. Meyerhof, C.G.: "The ultimate bearing capacity of foundations". Geotechnique, **2**(4): 301–332 (1951)
23. Rowe, P.W.: "The stress dilatancy relation for static equilibrium of an assembly of particles in contact". Proc. Roy. Soc., London, **A269**: 500–527 (1962)
24. de Josselin de Jong, G.: "Rowe's stress dilatancy relation based on friction". Geotechnique, **26**(3): 527–534 (1976)
25. Bolton, M.D.: "The strength and dilatancy of sands". Geotechnique, **36**(1): 65–78 (1986)
26. Salgado R., Bandini, P., and Karim, A.: "Shear strength and stiffness of silty sand". J. Geotech. and Geoenv. Eng., ASCE, Vol. **126**(5): 551–562 (2000)
27. Billam, J.: "Some aspects of the behaviour of granular material at high pressures". Stress strain behaviour of soils, (ed. R.H.V.Parry), Foulis, London, 69–80 (1972)
28. Singh, R.: Small strain stiffness and strength characteristics of ash. M.E. Thesis, Dept. Civil Eng., TIET, Patiala, 2002
29. Perkins, S.W., and Madson, C.R.: "Bearing capacity of shallow foundations on sand: A relative density approach". J. Geotech. and Geoenv. Eng., ASCE, Vol. **126**(6): 521–529 (2000)
30. Trivedi, A., and Sud, V.K.: "Collapse behavior of coal ash". J. Geotech. and Geoenv. Eng., ASCE, Vol. **130**(4): 403–415 (2004)